Energy Materials

Supplementary Materials

Improved interfacial li-ion transport in composite polymer electrolytes via surface modification of LLZO

Michael J. Counihan[1], Jungkuk Lee[2], Priyadarshini Mirmira[3], Pallab Barai[2], Meghan E. Burns[1,4], Chibueze V. Amanchukwu[3], Venkat Srinivasan[5], Yuepeng Zhang[2], Sanja Tepavcevic[1,*]

[1]Materials Science Division, Argonne National Laboratory, Lemont, IL 60439, USA.
[2]Applied Materials Division, Argonne National Laboratory, Lemont, IL 60439, USA.
[3]Pritzker School of Molecular Engineering, University of Chicago, Chicago, IL 60637, USA.
[4]Department of Chemistry, University of Chicago, Chicago, IL 60637, USA.
[5]Chemical Sciences and Engineering Division, Argonne National Laboratory, Lemont, IL 60439, USA.

[*]**Correspondence to:** Dr. Sanja Tepavcevic, Materials Science Division, Argonne National Laboratory, 9700 S Cass Ave, Lemont, IL, 60439, USA. E-mail: sanja@anl.gov

Table of Contents

Table S2. Fit Values for Modeling of Experimental Composite Data

Table S3 – Model Parameters

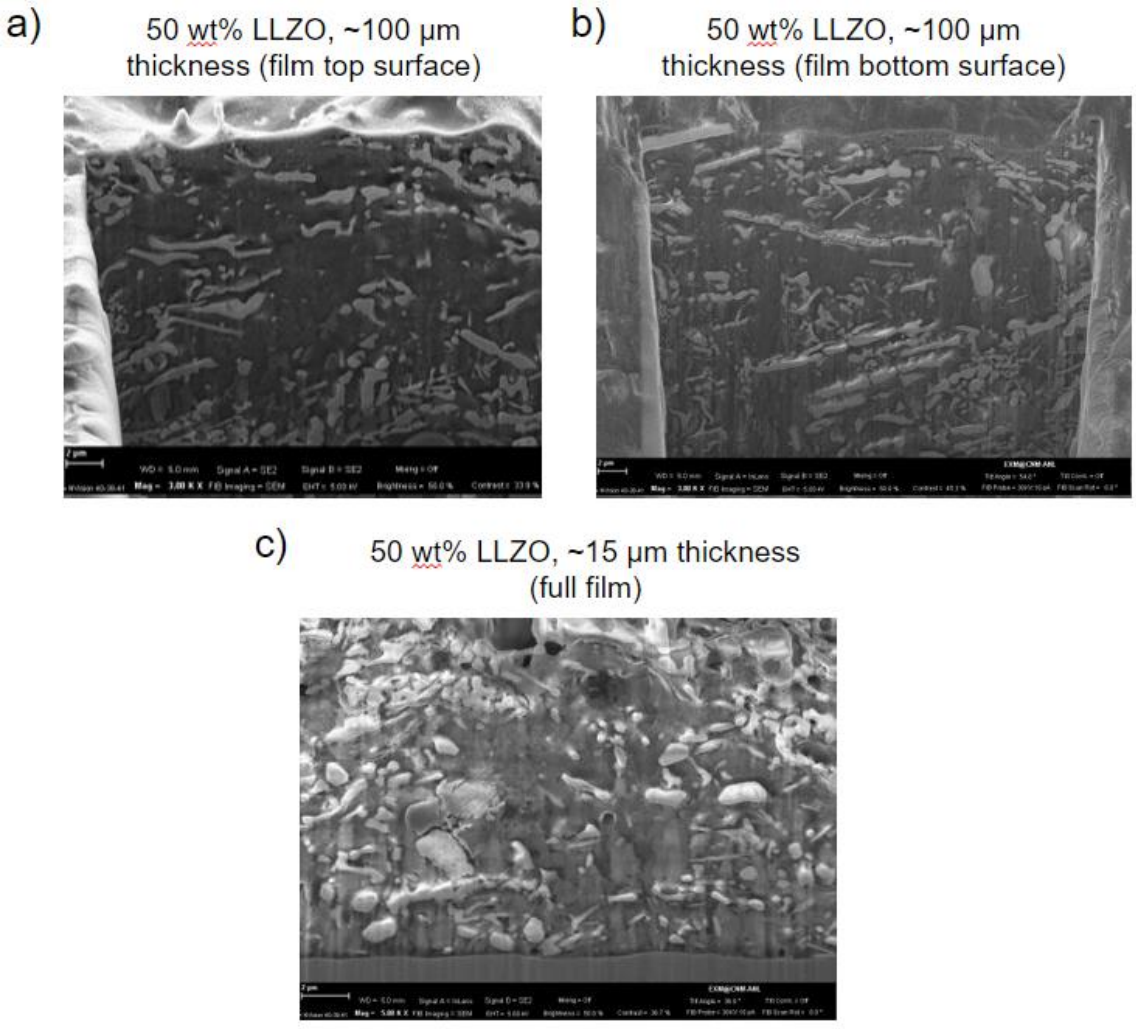

Figure S1. Cross-section SEM images of thick and thin composite membranes with uniform fiber distribution prepared by slot-die coating.

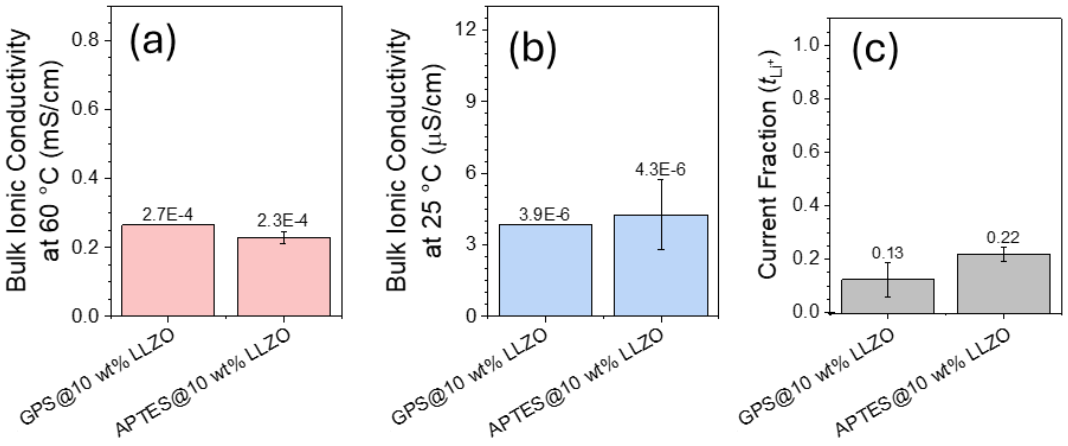

Figure S2. Bulk ionic conductivity at a) 60 °C and b) 25 °C, and c) transference number of composite membrane with GPS modified LLZO and APTES modified LLZO.

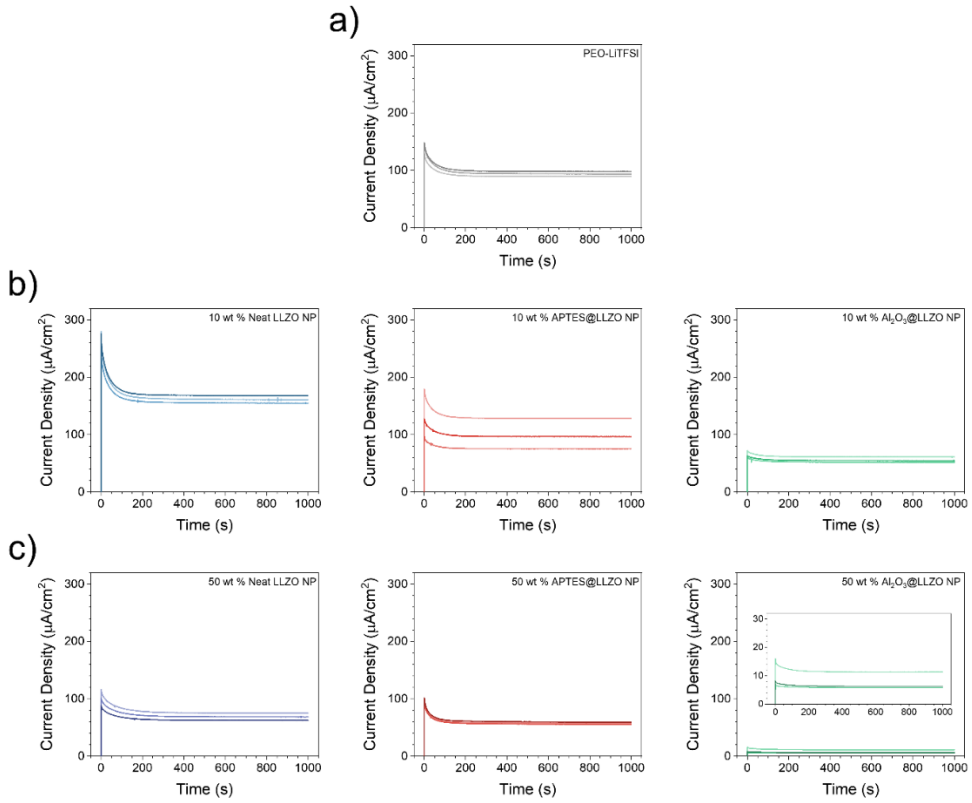

Figure S3. Chronoamperograms used for transference number calculations for a) PEO-LiTFSI, b) 10 wt % Neat LLZO NP, APTES@LLZO NP, and Al_2O_3@LLZO NP, and c) 50 wt % Neat LLZO NP, APTES@LLZO NP, and Al_2O_3@LLZO NP electrolytes. Results from three different cells are presented for each electrolyte. The applied bias was +50 mV, and the temperature was 60 °C.

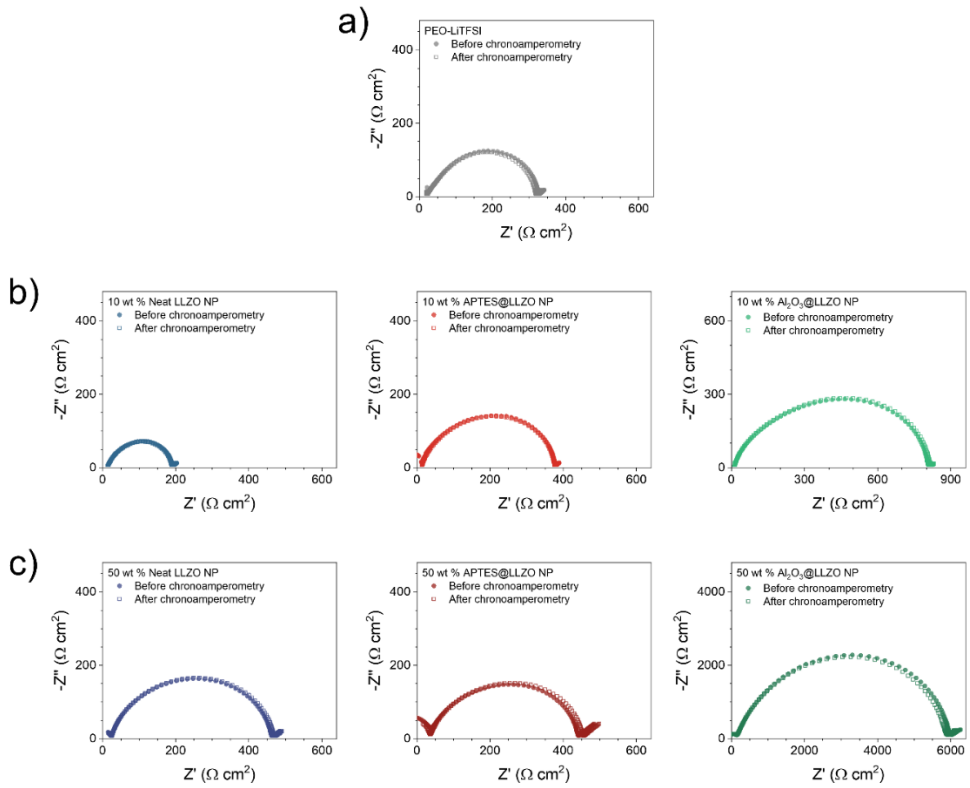

Figure S4. Representative Nyquist plots for a) PEO-LiTFSI, b) 10 wt % Neat LLZO NP, APTES@LLZO NP, and Al_2O_3@LLZO NP, and c) 50 wt % Neat LLZO NP, APTES@LLZO NP, and Al_2O_3@LLZO NP. Plots showed spectra taken before (solid circles) and after (open rectangles) chronoamperometry at 60 °C for transference number calculations.

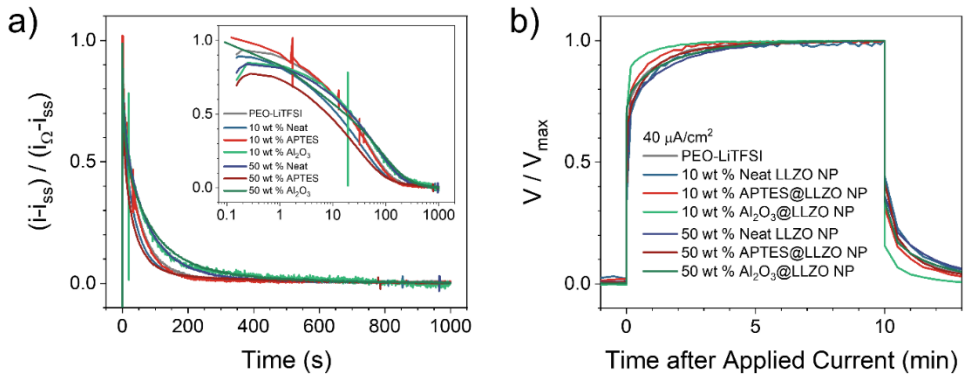

Figure S5. a) Normalized chronoamperograms from representative cells with the seven different electrolytes at 60 °C, +50 mV applied bias. The Ohmic initial current defined as $i_\Omega = V_{applied} / (R_b + R_{AnodeInt})$ was used to normalize the data following the method used by Chintapalli et al., *Macromolecules* **2016**, *49* (9), 3508–3515. Inset shows the data with logarithmic time scale. b) Normalized galvanostatic voltage profiles at 40 μA/cm^2 for the electrolytes.

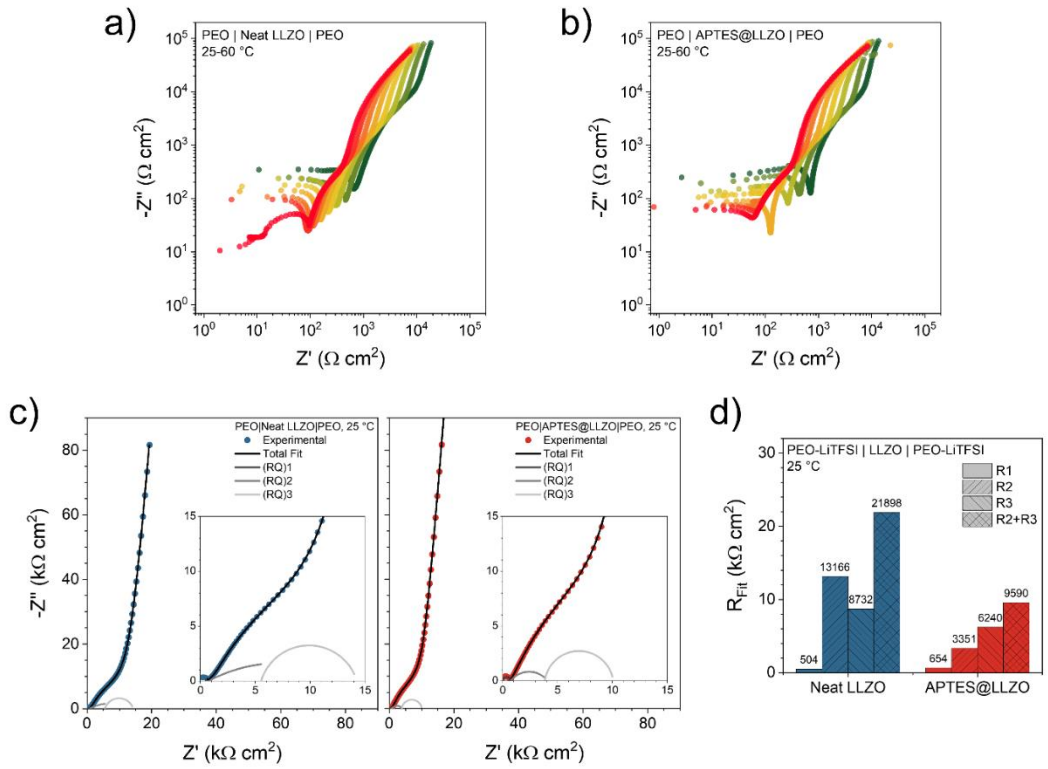

Figure S6. Nyquist plots (shown with dual logarithmic axes for clarity) of a) PEO-LiTFSI|Neat LLZO Pellet|PEO-LiTFSI and b) PEO-LiTFSI | APTES@LLZO Pellet | PEO-LiTFSI trilayer cells from **Figure 4** from 25 °C (green) to 60 °C (red). c) Nyquist plots of PEO-LiTFSI|LLZO|PEO-LiTFSI trilayer cells at 25 °C with Neat LLZO (top) and APTES@LLZO (bottom) pellets. Grayscale lines show semicircles from each fit R-CPE element. d) Fit resistances of the cells at 60 °C based on the equivalent circuit in **Figure 4c**.

Table S1. Chemical composition of LLZO NP, APTES@LLZO NP and LLZO NF

	LLZO NP	**APTES@LLZO NP**	**LLZO NF**
Li	5.99	4.68	6.4
Al	0.21	0.21	0.33
La	3.0	3.0	3.0
Zr	1.86	1.87	1.9

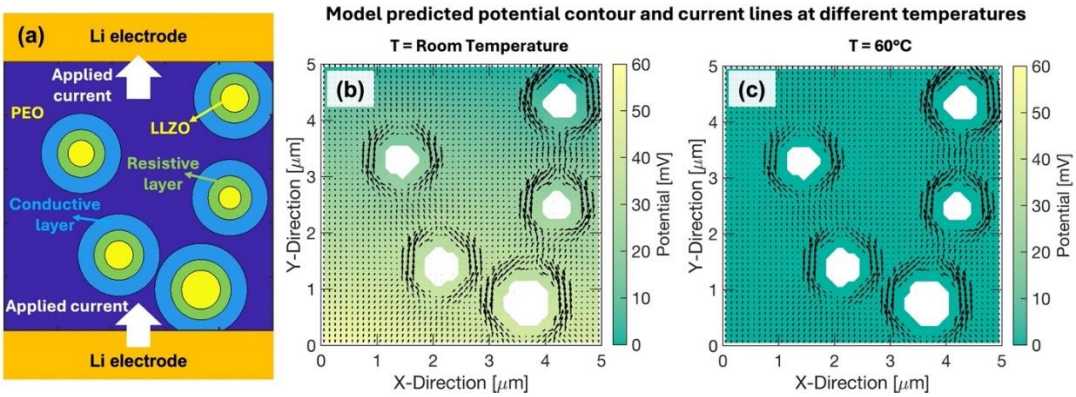

Figure: S7. (a) Schematic representation of the PEO/LLZO composite electrolyte with the resistive and conductive interphase layers located around the ceramic particles. In this particular representation, the LLZO content is assumed to be 10 wt %. The electrolyte is sandwiched between two lithium metal electrodes, and current is passed from the bottom to the top. (b – c) Potential contour and current arrow plots obtained at two different temperatures, (b) Room temperature, and (c) 60°C. Due to the lower conductivity of the polymer and the interphase layers at room temperature conditions, the potential gradient in (b) is much higher than that observed in (c) under 60°C. However, the current arrows clearly indicate that irrespective of the temperature of operation, majority of the current prefers to flow through the conductive region. No current flows through the LLZO particles, and the flow of current along the resistive interphase region is also negligible.

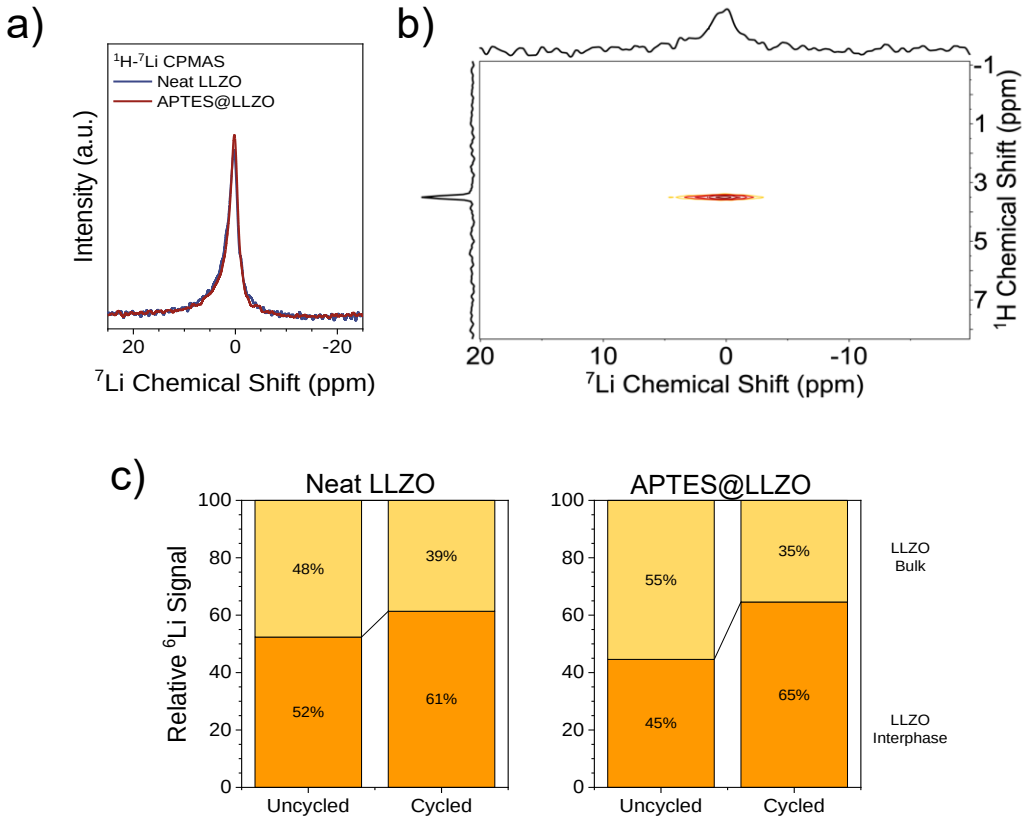

Figure S8. a) ^{7}Li- ^{1}H cross polarization NMR of neat and silane coated LLZO-PEO composites. b) Relative amounts of LLZO Interphase and LLZO Bulk signals quantified from ^{6}Li NMR.

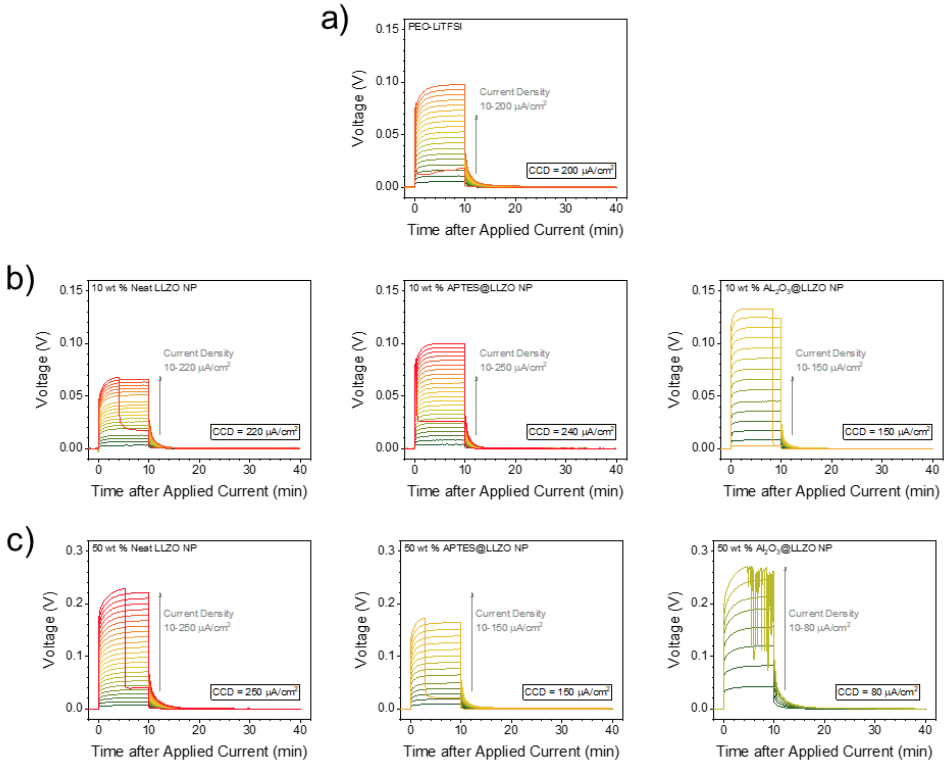

Figure S9. Galvanostatic cycling profiles overlaid with increasing current density for representative cells of a) PEO-LiTFSI, b) 10 wt % Neat LLZO NP, APTES@LLZO NP, and Al_2O_3@LLZO NP, and c) 50 wt % Neat LLZO NP, APTES@LLZO NP, and Al_2O_3@LLZO NP electrolytes.

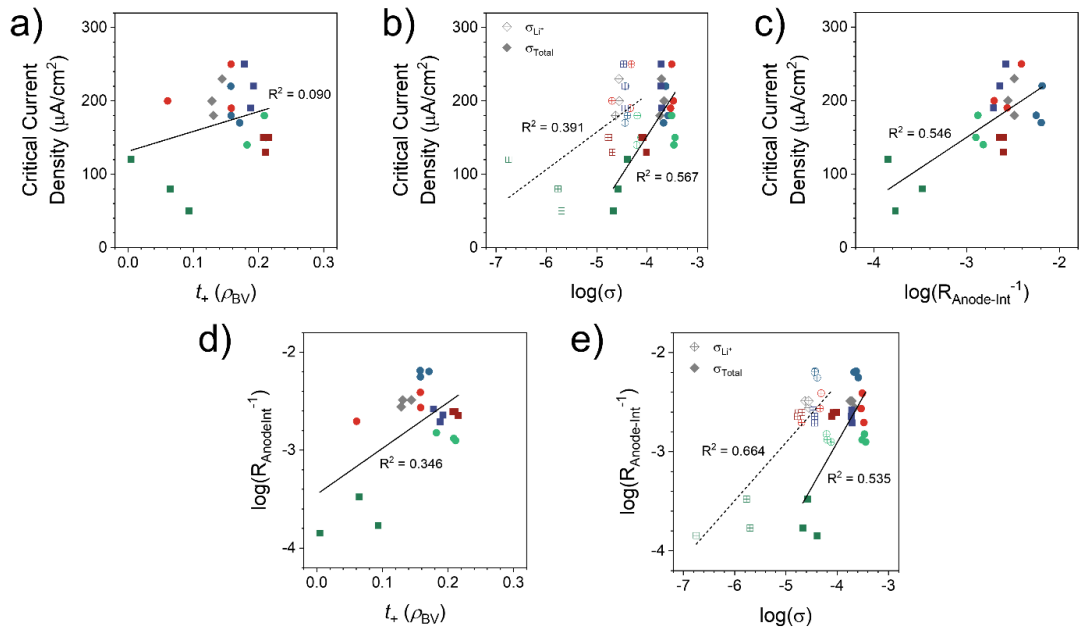

Figure S10. a) Correlation between CCD and estimated transference number. b) Correlation between CCD and total ionic and Li^+ conductivities. c) Correlation between CCD and $R_{AnodeInt}$. d) Correlation between $R_{AnodeInt}$ and estimated transference number. e) Correlation between $R_{Anode\text{-}Int}$ and total ionic and Li^+ conductivities. All points are individual cells. Reported R^2 values are from linear regressions of the presented data.

Table S2. Fit values used to model conductivities and transference numbers in **Figure 5.**

	$t_{Intph,Resistive}$	$\frac{\kappa_{Intph,Resistive}}{\kappa_{PEO}}$	$t_{Intph,Conductive}$	$\frac{\kappa_{Intph,Conductive}}{\kappa_{PEO}}$	$t_+^{Interphase}$	t_+^{Bulk}
Neat LLZO	200 nm	0.031	300 nm	10.0	0.264	0.184
APTES @ LLZO	250 nm	0.1	700 nm	4.0	0.574	0.114
Al_2O_3@ LLZO	400 nm	0.1	400 nm	9.0	0.0	0.194
PEO-LiTFSI	--	--	--	--	--	0.134

Description of the Two-Interphase Composite Model

Effective conductivity and transference number within the composite electrolyte is estimated using mathematical techniques. The composite electrolyte consists of LLZO based ceramic particles or fibers, and PEO based polymer matrix. LiTFSI mixed with PEO acts as the ion carrying electrolyte salt. Single ion conducting behavior is assumed within the LLZO phase where potential gradient induced migration drives the movement of ions. Ion transport in PEO is assumed to follow the theory of binary electrolytes, where both migration and diffusion governs the movement of ions. An interfacial resistance between the PEO polymer and the LLZO ceramic phase is also assumed that helps to control the propensity of ion transport from the polymer to the ceramic phase (and vice versa). Higher magnitude of polymer/ceramic interfacial resistance prevents facile transport of ions from one phase to the other, whereas smaller magnitude of the interfacial resistance facilitates easy transfer of ions. In general, the LLZO ceramic is expected to demonstrate higher conductivity than the PEO polymer, and transport of ions through the minimum resistance pathway should determine the final transport route taken by the ions within the composite electrolyte.

It is hypothesized that different interphase layers can form around LLZO ceramics that can influence the transport of ions within the adjacent polymer phase. In order to capture the variation in ionic transport within the interphase regions, two different polymer/ceramic interphase domains are modeled. The first interphase is adjacent to the LLZO based ceramic particles, which tries to restrict the mobility of polymer chains, and effectively results in a lower ionic conductivity than the bulk of the polymer. The other interphase layer is farther away from the ceramic phase and acts as a plasticized domain with higher polymer chain mobility that effectively leads to an increase in ionic conductivity than the bulk of PEO. The thickness, conductivity, and transference number of these two interphase domains are considered as fitting parameters, and the adopted values are those that provides the best fit with the experimental observations.

The following governing equations, along with appropriate boundary conditions, are solved for estimating the effective conductivities and transference numbers within the polymer/ceramic composite electrolyte domain[1,2].

Governing equations for LLZO ceramic phase: Ion transport within LLZO particles and/or fibers are assumed to occur through a single ion conducting mechanism, which indicates ion transport only by migration under the influence of potential gradients. No concentration gradient evolves within the ceramic phase. The following equation is solved for capturing the potential distribution within LLZO ceramics:

$$\nabla(\kappa_{\mathrm{LLZO}}\nabla\phi_{\mathrm{LLZO}}) = 0 \tag{S1}$$

Here, κ_{LLZO} indicates the ionic conductivity and ϕ_{LLZO} denotes the electrolyte potential within the ceramic phase. Since no LLZO is assumed to touch the Li electrode, no boundary condition is assigned associated with the LLZO domain. Only PEO/LLZO interfacial conditions are associated at the boundary of the LLZO domains, which will be discussed later.

Governing equations for the PEO polymer phase: Transport of ions within the PEO polymer occurs through both migration and diffusion. Local current in the PEO phase (i_{PEO}) is given by the following expression:

$$i_{\mathrm{PEO}} = -\kappa_{\mathrm{PEO}}\nabla\phi_{\mathrm{PEO}} + \frac{2\kappa_{\mathrm{PEO}}RT}{F}\left(1 - t_{+,\mathrm{PEO}}\right)\left(1 + \frac{d\ln f_{\pm}}{d\ln c_{\mathrm{PEO}}}\right)\nabla(\ln c_{\mathrm{PEO}}) \tag{S2}$$

where, κ_{PEO} indicates conductivity within the PEO polymer, ϕ_{PEO} is the electrolyte potential within PEO, R is the universal gas constant, T denotes temperature, F is the Faraday constant, $t_{+,\mathrm{PEO}}$ is the transference number in PEO electrolyte, c_{PEO} is the salt concentration within PEO polymer phase, and $f_{\pm}$ is the activity coefficient. Conservation of charge within the PEO phase is satisfied by solving the following equation within the bulk of the electrolyte:

$$\nabla\cdot(i_{\mathrm{PEO}}) = 0 \tag{S3}$$

Time dependent variation in lithium salt concentration within the PEO phase is captured by solving the following governing equation:

$$\frac{\partial c_{\mathrm{PEO}}}{\partial t} = \nabla\left(D_{\mathrm{PEO}}\left(1 - \frac{d\ln c_0}{d\ln c_{\mathrm{PEO}}}\right)\nabla c_{\mathrm{PEO}}\right) - \nabla\left(\frac{i_{\mathrm{PEO}}t_{+,\mathrm{PEO}}}{F}\right) \tag{S4}$$

Here, t indicates time, D_{PEO} is the binary salt diffusivity within the PEO polymer phase, c_0 indicates the solvent concentration, and the other symbols were explained earlier. In order to simplify the analysis, the activity coefficient is assumed to be constant ($f_{\pm} = \mathrm{const.}$) such that the thermodynamic factor can be simplified to unity, $(1 + d\ln f_{\pm}/d\ln c_{\mathrm{PEO}}) = 1.0$. The change in solvent concentration with salt is also assumed to be zero, such that $(1 - d\ln c_0/d\ln c_{\mathrm{PEO}}) = 1.0$. The lithium salt diffusivity within PEO is also assumed to be constant ($D_{\mathrm{PEO}} = \mathrm{const.}$).

However, the two interphase regions adjacent to the LLZO ceramics can demonstrate different transference numbers, which indicates non-zero gradient of the transference number $\left(\nabla t_{+,\mathrm{PEO}} \neq 0\right)$.

PEO/LLZO interfacial current: The reaction current at the interface between the PEO polymer and the LLZO ceramics $\left(i_{\mathrm{PEO/LLZO}}\right)$ is estimated from the following expression:[2]

$$i_{\mathrm{PEO/LLZO}} = \frac{\phi_{\mathrm{LLZO}} - \phi_{\mathrm{PEO}}}{R_{\mathrm{PEO/LLZO}}} \tag{S5}$$

where, $R_{\mathrm{PEO/LLZO}}$ denotes the interfacial resistance between PEO polymer and the LLZO ceramic phase. The diffusive lithium flux at the PEO/LLZO interface $\left(N_{\mathrm{diff,PEO/LLZO}}\right)$ can be written as (at the PEO side):

$$N_{\mathrm{diff,PEO/LLZO}} = \left(1 - t_{+,\mathrm{PEO}}\right) i_{\mathrm{PEO/LLZO}} / F \tag{S6}$$

Note that there is no diffusive flux of lithium at the LLZO side due to the single ion conducting behavior of the ceramic particles.

Boundary conditions: Since the analysis is being conducted in a two-dimensional (2D) domain, there exist four different boundaries where boundary conditions need to be applied. The current is applied along the top-bottom direction, and the left-right boundaries experience zero current boundaries. For the potential solve, the following expressions are used on the left and right sides where zero current is applied:

$$i_{\mathrm{PEO}}\big|_{\substack{\mathrm{left} \\ \mathrm{right}}} = 0 \tag{S7}$$

Zero potential is applied at the top boundary: $\phi_{\mathrm{PEO}}|_{\mathrm{top}} = 0$ (S8)

Constant current is applied at the bottom boundary for the potential solve:

$$i_{\mathrm{PEO}}|_{\mathrm{bottom}} = I_{\mathrm{appleid}} \tag{S9}$$

where, I_{appleid} indicates the applied current density. Note that the no LLZO is allowed to touch the lithium electrode or the boundary of the electrolyte domain at the top, bottom, left, or right boundaries. The total lithium flux $\left(N_{\mathrm{Li^+,PEO}}\right)$ at the boundaries can be written as:

$$N_{\mathrm{Li^+,PEO}}\big|_{\substack{\mathrm{left} \\ \mathrm{right}}} = 0 \qquad \text{and} \qquad N_{\mathrm{Li^+,PEO}}\big|_{\substack{\mathrm{top} \\ \mathrm{bottom}}} = \pm\frac{I_{\mathrm{applied}}}{F} \tag{S10}$$

Note that the total lithium flux contains both the migration and diffusion components, and the diffusive component is extracted by subtracting the migration component from the total lithium flux.

All the above-mentioned equations are solved using a Finite Volume Methodology (FVM), where the two polymer and ceramic domains are modeled using a single domain approach, but with distinct properties. The two resistive and conductive interphases around the LLZO ceramics are also captured using the same single domain scheme, but through the adoption of different conductivity and transference numbers. The diffusivity of lithium salt within PEO are assumed to be same in bulk and the interphase domains. No special assumption is added while modeling the APTES or Al_2O_3 coated LLZO particles/fibers, the same polymer/ceramic composite is simulated with similar two interphase domains. However, different thickness, conductivity, and transference numbers of the two interphase layers needs to be adopted for obtaining the best fit with the experimental observations for neat-LLZO, APTES-LLZO and Al_2O_3-LLZO.

Computational estimation of the effective conductivity (κ_{eff}) and the PEO/LLZO composite electrolyte is conducted in a $5\mu m \times 5\mu m$ computational domain by applying constant current $\left(I_{\text{applied}}\right)$ between the top and bottom ends of the electrolyte and by measuring the voltage drop across the thickness direction (denoted as ΔV). The final conductivity is estimated as:

$$\kappa_{\text{eff}} = \frac{I_{\text{applied}} \cdot L}{\Delta V} \tag{S11}$$

where, L indicates thickness of the solid electrolyte domain. The generated computational domain contains the bulk PEO phase, LLZO ceramic fibers, and the resistive and conductive interphase regions adjacent to the LLZO. For the estimation of conductivity, voltage drop at very small time, for example less than a fraction of a second ($< 0.1s$), is considered, where no significant evolution of the concentration gradient can occur. However, for estimating the transference number, the simulation is run long enough till steady state is reached. The effective transference number $\left(t_{+,\text{i}}\right)$ of a particular cross section is estimated by averaging out the transference number at different locations weighted by the local current distribution at steady state.

$$t_{+,\text{i}} = \frac{\sum t_{+,\text{n}} \cdot i_{\text{loc,n}}}{\sum i_{\text{loc,n}}} \tag{S12}$$

Here, $t_{+,\mathrm{n}}$ and $i_{\mathrm{loc,n}}$ denotes the transference number and the local current at a particular location, which can be the LLZO ceramic, or PEO bulk, or either of the two interphase regions. Transference number of the entire computational domain $\left(t_{+,\mathrm{eff}}\right)$ can be estimated by averaging out the transference numbers at multiple such cross sections. The following equation can be used for estimating the transference number of the entire composite electrolyte:

$$t_{+,\mathrm{eff}} = \frac{\Sigma t_{+,i}}{\#\ of\ cross\ sections} \tag{S13}$$

All these methodologies of estimating the effective conductivity and transference number of composite electrolytes were mentioned in previous publications[2].

Table S3. The following list of parameters are used while estimating the effective conductivity and transference number of the PEO/LLZO composite.

Model parameters	**Value**	**Ref.**
Dimension of computational domain	$5\ \mu\mathrm{m} \times 5\ \mu\mathrm{m}$	Used for faster execution of the model with fine enough spatial resolution
Spatial resolution	$100\ \mathrm{nm}$	Sufficient for capturing all the microstructural details
Conductivity of LLZO	$0.5\ \mathrm{S/m}$	[3]
Conductivity of PEO at 30ºC	$5.91 \times 10^{-5}\ \mathrm{S/m}$	Measured
Conductivity of PEO at 60ºC	$1.97 \times 10^{-2}\ \mathrm{S/m}$	Measured
Transference number in PEO	0.134	Measured
Transference number in LLZO	1.0	Due to single ion conducting behavior
Diffusivity of Li-salt in PEO	$8.0 \times 10^{-12}\ \mathrm{m^2/s}$	[4]
Charge transfer resistance between PEO and LLZO	$4000\ \Omega \cdot \mathrm{cm^2}$	Assumed large number to prevent Li-ion transfer from PEO to LLZO

REFERENCES

1. Newman, J.S. and K.E. Thomas-Alyea, *Electrochemical systems*. 3rd ed. 2004, Hoboken, N.J.: J. Wiley. xx, 647 p.

2. Kim, H.K., et al., *Transport and mechanical behavior in PEO-LLZO composite electrolytes.* Journal of Solid State Electrochemistry, 2022. **26**(9): p. 2059-2075.

3. Samson, A.J., et al., *A bird's-eye view of Li-stuffed garnet-type LiLaZrO ceramic electrolytes for advanced all-solid-state Li batteries.* Energy & Environmental Science, 2019. **12**(10): p. 2957-2975.

4. Mullin, S.A., et al., *Salt Diffusion Coefficients in Block Copolymer Electrolytes.* Journal of the Electrochemical Society, 2011. **158**(6): p. A619-A627.